NBSIR 75-829

RADIATION CHARACTERISTICS OF DIPOLE SOURCES LOCATED INSIDE A RECTANGULAR, COAXIAL TRANSMISSION LINE

John C. Tippet
David C. Chang
University of Colorado

Sponsored by:
Electromagnetics Division
Institute for Basic Standards
National Bureau of Standards
Boulder, Colorado 80302

January 1976

Prepared for:
Electronics Systems Division (AFSC)
Hanscom Air Force Base, Mass. 01731

NBSIR 75-829

RADIATION CHARACTERISTICS OF DIPOLE SOURCES LOCATED INSIDE A RECTANGULAR, COAXIAL TRANSMISSION LINE

John C. Tippet
David C. Chang
University of Colorado

Sponsored by:
Electromagnetics Division
Institute for Basic Standards
National Bureau of Standards
Boulder, Colorado 80302

January 1976

Prepared for:
Electronics Systems Division (AFSC)
Hanscom Air Force Base, Mass. 01731

U.S. DEPARTMENT OF COMMERCE, Rogers C. B. Morton, Secretary
James A. Baker, III, Under Secretary
Dr. Betsy Ancker-Johnson, Assistant Secretary for Science and Technology

NATIONAL BUREAU OF STANDARDS, Ernest Ambler, Acting Director

CONTENTS

		Page
	FOREWORD	iv
1.	INTRODUCTION	1
2.	PARAMETERS CHARACTERIZING A TEM CELL	2
3.	APPROXIMATE EXPRESSIONS FOR THE CAPACITANCE AND CHARACTERISTIC IMPEDANCE	5
4.	RADIATION RESISTANCE OF ELECTRIC AND MAGNETIC DIPOLES IN A TEM CELL	9
5.	SUMMARY AND CONCLUDING REMARKS	13
6.	REFERENCES	16
APPENDIX A:	Calculation of the Capacitance of a TEM Cell	17
APPENDIX B:	Calculation of the Electric Field Distribution Inside a TEM Cell	21
APPENDIX C:	Numerical Evaluation of Complete Elliptic Integrals and Jacobian Elliptic Functions	29

FOREWORD

This report describes theoretical analyses of Transverse Electromagnetic (TEM) Transmission cells developed at the National Bureau of Standards. The effort is part of a program sponsored by the Electronic Systems Division, Hanscom Air Force Base, under Contract number Y75-917 with the National Bureau of Standards (NBS). The purpose of this effort is to evaluate the use of TEM cells for measuring total RF power radiated by a small electronic device.

The theoretical analyses were developed by staff from the University of Colorado under contract with NBS. Myron L. Crawford of the Electromagnetics Division was the technical monitor for NBS and Charles E. Wright of the Electronics Systems Division was the technical monitor for the Air Force. The period of performance covered by this report extends from May 1975 to October 1975.

Results of these analyses include expressions for the capacitance and characteristic impedance of a cell, the electric field distribution inside a cell, and the radiation resistance of electric and magnetic dipoles in a cell. These results are prerequisite to determining the radiation characteristics of a device under test relative to its operational environment or to its operation in a free space environment.

RADIATION CHARACTERISTICS OF DIPOLE SOURCES LOCATED INSIDE A RECTANGULAR, COAXIAL TRANSMISSION LINE

When making EMC measurements inside a shielded enclosure, the radiation characteristics of the device being tested changes. In this report the change in radiation resistance of dipole sources located inside a National Bureau of Standards TEM transmission cell is determined. In many cases a practical device can be modeled by dipole sources. In these cases, the analysis allows one to predict the device's radiation characteristics in other environments, e.g., free space.

Key words: EMC measurements; radiation resistance; rectangular coax; shielded strip line; TEM cell.

1. INTRODUCTION

There are currently many researchers interested in developing a method of measuring the radiated EM emissions and EM susceptibility of electronic equipment [1]. At the National Bureau of Standards work is progressing on the design and experimental evaluation of a TEM transmission cell for this purpose. A typical NBS cell consists of a section of rectangular coaxial transmission line tapered at each end to connect to standard 50 Ω coaxial line as shown in figure 1.

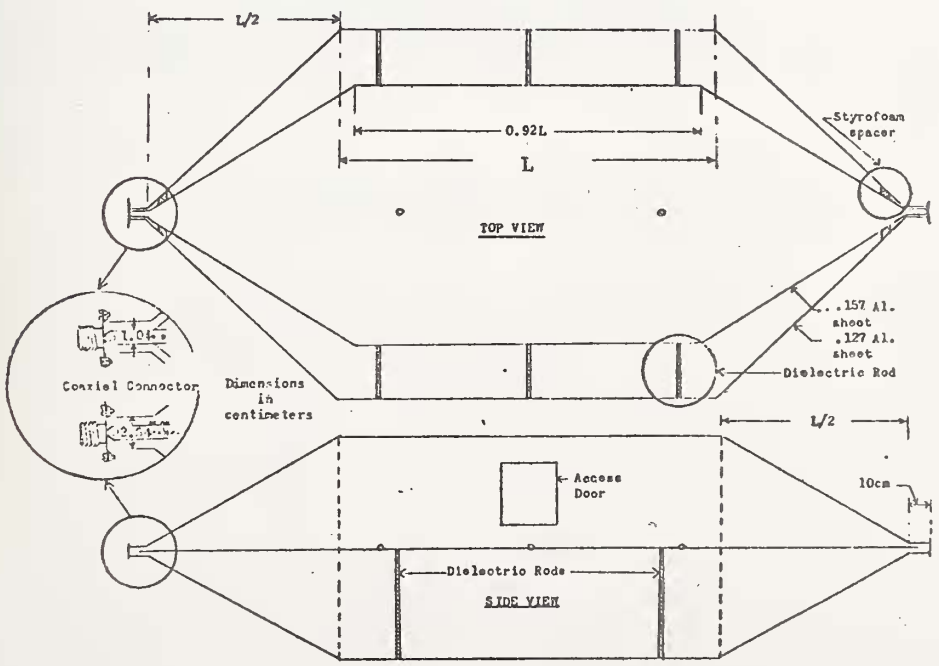

Figure 1. Design for rectangular TEM transmission cell.

To minimize reflections, the cell is designed to have a nominal characteristic impedance of 50 Ω. The description, design, and evaluation of these cells is described in reference [2].

In order to interpret the measurements made in this cell, a knowledge of the propagating TEM mode is required. This report contains a theory for calculating some basic properties of the TEM mode. These include: 1) capacitance; 2) characteristic impedance; and 3) electric field distribution inside the cell.

Once we possess a basic knowledge of the TEM mode, we can study the radiation characteristics of some simple sources located inside the cell. Since these characteristics will not be the same as if the source were located in free space, we need to determine the effect the TEM cell has on the radiation resistance of the source. This will allow measurements made in the TEM cell to be correctly interpreted for sources in other environments such as free space.

The power radiated by and the radiation resistance of both electric and magnetic dipoles located in the TEM cell are derived and compared to their values in free space. We indicate how these expressions can be used to determine both the magnitudes and directions of the respective dipoles through measurements made in the TEM cell.

2. PARAMETERS CHARACTERIZING A TEM CELL

The TEM cell is basically a rectangular, coaxial transmission line as shown in figure 2.

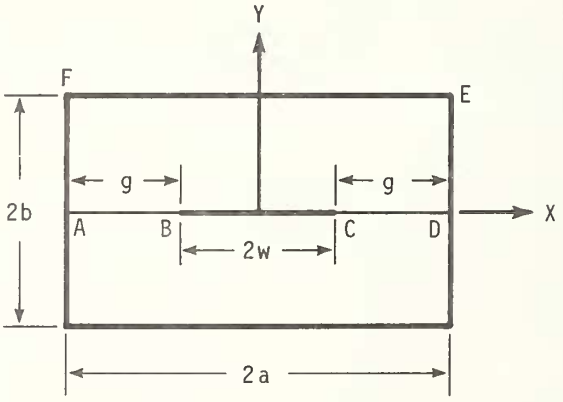

Figure 2. Cross-section of a TEM cell.

In order to understand how an electromagnetic wave can be guided by this structure, a brief review of the results from standard transmission line theory is presented.

Any multi-conductor system, of which the TEM cell is one, can propagate at least one TEM mode. This mode has many unique properties, not the least of which is that it has no lower cut-off frequency. That is, the TEM mode can propagate through the guide at frequencies all the way down to DC. Another characteristic property of the TEM mode (as its name implies) is that the electric and magnetic field components of this mode lie totally in the transverse plane (i.e., $E_z = H_z = 0$). In the transverse plane, the electric field satisfies Laplace's equation: $\nabla_t^2 \bar{E} = 0$, which in the case of the TEM cell reduces to: $(\frac{\partial^2}{\partial x^2} + \frac{\partial^2}{\partial y^2})\bar{E}(x,y) = 0$. This means that the transverse field distribution can be obtained from the solution of a related static problem. The magnetic field is easily obtained from the electric field as

$$\hat{\bar{H}}^{\pm} = \pm \frac{\bar{a}_z \times \hat{\bar{E}}^{\pm}}{\eta_o} \tag{2.1}$$

where

$\hat{\bar{E}}^{\pm} = \bar{E}(x,y)e^{jwt \mp \gamma z}$;

$\hat{\bar{H}}^{\pm} = \bar{H}(x,y)e^{jwt \mp \gamma z}$;

$\eta_o = \sqrt{\frac{\mu_o}{\varepsilon_o}}$;

μ_o is the magnetic permeability;

ε_o is the dielectric permittivity;

γ is the propagation constant;

and $\bar{a}_z$ is a unit vector in the z direction.

The total fields are then given by:

$$\bar{E} = \mathrm{Re}[\hat{\bar{E}}^{+} + \hat{\bar{E}}^{-}] \tag{2.2}$$

and

$$\bar{H} = \mathrm{Re}[\hat{\bar{H}}^{+} + \hat{\bar{H}}^{-}] \tag{2.3}$$

Many times, it is desirable to characterize TEM waves in terms of the voltage and current on the line instead of the field quantities, $\bar{E}$ and $\bar{H}$. The voltage and current are given by the following equations:

$$\hat{V}(z) = \hat{V}_m^{+}e^{-\gamma z} + \hat{V}_m^{-}e^{\gamma z} \tag{2.4}$$

$$\hat{I}(z) = \hat{I}_m^{+}e^{-\gamma z} + \hat{I}_m^{-}e^{\gamma z} \tag{2.5}$$

where

$$\hat{V}_m^{\pm} = -\int_p \hat{\bar{E}}^{\pm} \cdot \overline{d\ell} \tag{2.6}$$

and

$$\hat{I}_m^{\pm} = \oint_\ell \hat{\bar{H}}^{\pm} \cdot \overline{d\ell} \tag{2.7}$$

p is any path connecting the two conductors in a constant cross-sectional plane, and ℓ is a closed path encircling the inner conductor. $\hat{V}_m$ and $\hat{I}_m$ are related by a constant which is called the characteristic impedance, Z_o of the line, and is given by:

$$Z_o = \pm \frac{\hat{V}_m^{\pm}}{\hat{I}_m^{\pm}} = \pm \frac{\hat{V}_m^{\pm}}{\oint_{\ell} \frac{\bar{a}_z \times \bar{\hat{E}}^{\pm}}{\eta_o} \cdot \overline{d\ell}} \tag{2.8}$$

Thus, eq. (2.5) may be written:

$$\hat{I}(z) = \frac{\hat{V}_m^{+}}{Z_o} e^{-\gamma z} - \frac{\hat{V}_m^{-}}{Z_o} e^{\gamma z} \tag{2.9}$$

If one measures the amplitudes of the forward and backward voltage waves, $\hat{V}_m^{\pm}$, then, with a knowledge of the characteristic impedance, eqs. (2.4) and (2.9) determine the voltage and current anywhere on the line.

The characteristic impedance, Z_o, can also be expressed in terms of the distributed capacitance per unit length of the transmission line, C_o as follows:

$$Z_o = \frac{1}{v\, C_o} \tag{2.10}$$

where $v = \frac{1}{\sqrt{\mu_o \varepsilon_o}}$ is the phase velocity.

Thus, a knowledge of the distributed capacitance, C_o, completely determines the characteristic impedance.

The capacitance of the TEM cell can be obtained analytically using the method of conformal transformation. The details of the analysis are contained in Appendix A where it is shown that the capacitance per unit length, C_o, is given by:

$$\frac{C_o}{\varepsilon_o} = 2 \frac{K(\lambda)}{K(\lambda')} \tag{2.11}$$

where $K(\lambda)$ and $K(\lambda')$ are complete elliptic integrals of the first kind of modulus λ and λ' respectively [3]. λ' is termed the complementary modulus and is related to λ by:

$$\lambda' = [1 - \lambda^2]^{\frac{1}{2}} \tag{2.12}$$

The modulus, λ', is given by:

$$\lambda' = k' \left[\frac{\text{sn } \xi}{\text{cn } \xi}\right]^2 \tag{2.13}$$

where $\xi = mg$ and sn ξ and cn ξ are Jacobian elliptic functions of modulus k [4]. As shown in figure 2, g = a-w is the width of the gap between the center septum

and the side wall. k' is the complementary modulus to k defined analogously to eq. (2.12), and m is given by:

$$m = \frac{K(k')}{b} \tag{2.14}$$

k, and thus, k' can be determined from the requirement that:

$$\frac{K(k)}{K(k')} = \frac{2a}{b} \tag{2.15}$$

where K(k) and K(k') are complete elliptic integrals of the first kind of modulus k and k' respectively. We note that in reference [5] the value of k^2 is tabulated for a given ratio, K(k')/K(k).

Using eq. (2.10), the characteristic impedance is then found to be:

$$\frac{Z_o}{\eta_o} = \frac{1}{2}\frac{K(\lambda')}{K(\lambda)} \tag{2.16}$$

where η_o is the intrinsic impedance of free space. Equations (2.11) and (2.16) are exact but are not easy to use. There is an efficient algorithm [6], however, for evaluating numerically the complete elliptic integrals appearing in eqs. (2.11) and (2.16); it is contained in Appendix C. In the next section, approximate formulas are derived for the capacitance and characteristic impedance.

3. APPROXIMATE EXPRESSIONS FOR THE CAPACITANCE AND CHARACTERISTIC IMPEDANCE

In view of the complete elliptic integrals appearing in the formulas in the last section, it is desirable to investigate the possibility of obtaining formulas which do not involve special functions, but nevertheless, yield numerical results sufficiently accurate to be of practical engineering use. We hope to obtain a formula which expresses the capacitance in terms of the dimensions, a, b, and w of the TEM cell, and which can thus be used to design TEM cells with a given characteristic impedance.

Since eqs. (2.11), (2.15), and (2.16) all involve ratios of complete elliptic integrals, the following approximation is particularly useful [7].

$$\frac{K(\delta)}{K(\delta')} \simeq \frac{1}{\pi} \ln\left(2\,\frac{1+\sqrt{\delta}}{1-\sqrt{\delta}}\right) \qquad (\delta^2 > \tfrac{1}{2}) \tag{3.1}$$

Using eq. (3.1) we can write approximate expressions for eqs. (2.15) and (2.11) respectively as follows:

$$\frac{2a}{b} \simeq \frac{1}{\pi} \ln\left(2\,\frac{1+\sqrt{k}}{1-\sqrt{k}}\right) \qquad (k^2 > \tfrac{1}{2}) \tag{3.2}$$

$$\frac{C_o}{\varepsilon_o} \simeq \frac{2}{\pi} \ln\left(2\,\frac{1+\sqrt{\lambda}}{1-\sqrt{\lambda}}\right) \qquad (\lambda^2 > \tfrac{1}{2}) \tag{3.3}$$

Equations (3.2) and (3.3) may be written alternatively as follows:

$$\frac{4a}{b} \simeq \frac{2}{\pi} \ln[2(1+\sqrt{k})^2(1+k)] - \frac{2}{\pi} \ln(1-k^2) \tag{3.4}$$

$$\frac{C_o}{\varepsilon_o} \simeq \frac{2}{\pi} \ln[2(1+\sqrt{\lambda})^2(1+\lambda)] - \frac{2}{\pi} \ln(1-\lambda^2) \tag{3.5}$$

Subtracting eq. (3.4) from eq. (3.5) we obtain:

$$\frac{C_o}{\varepsilon_o} - \frac{4a}{b} \cong \frac{2}{\pi} \ln\left(\frac{k'^2}{\lambda'^2}\right) + \frac{2}{\pi} \ln\left\{\left(\frac{1+\sqrt{\lambda}}{1+\sqrt{k}}\right)^2 \left(\frac{1+\lambda}{1+k}\right)\right\} \tag{3.6}$$

and substituting from eq. (2.13):

$$\frac{C_o}{\varepsilon_o} \cong 4\left(\frac{a}{b} + \frac{2}{\pi} \ln\left(\frac{cn\ \xi}{sn\ \xi}\right)\right) + \frac{2}{\pi} \ln\left\{\left(\frac{1+\sqrt{\lambda}}{1+\sqrt{k}}\right)^2 \left(\frac{1+\lambda}{1+k}\right)\right\} \tag{3.7}$$

In eq. (3.2), the restriction that $k^2 > \frac{1}{2}$ is equivalent to requiring $\frac{b}{2a} < 1$, since when $k^2 = \frac{1}{2}$, $K(k') = K(k)$. If we make the somewhat more stringent requirement that $\frac{b}{a} < 1$, which is equivalent to $k^2 > .97$, then eq. (3.7) may be further simplified by noting that for $k \simeq 1$, $cn\ \xi \simeq \text{sech}\ \xi$; $sn\ \xi \simeq \tanh\ \xi$, and $\xi \simeq \frac{\pi g}{2b}$. Thus,

$$\frac{C_o}{\varepsilon_o} \simeq 4\left(\frac{a}{b} - \frac{2}{\pi} \ln\left(\sinh\ \frac{\pi g}{2b}\right)\right) - \frac{\Delta C}{\varepsilon_o} \tag{3.8}$$

where

$$\frac{\Delta C}{\varepsilon_o} = \frac{2}{\pi} \ln\left\{\left(\frac{1+\sqrt{k}}{1+\sqrt{\lambda}}\right)^2 \left(\frac{1+k}{1+\lambda}\right)\right\} \tag{3.9}$$

An alternate form of eq. (3.8) may be obtained by using the following identity:

$$\sinh\left(\frac{\pi g}{2b}\right) = \frac{e^{(\pi g/2b)}}{[1 + \coth(\frac{\pi g}{2b})]} \tag{3.10}$$

with the result:

$$\frac{C_o}{\varepsilon_o} \simeq 4\left(\frac{w}{b} + \frac{2}{\pi} \ln\left(1 + \coth\ \frac{\pi g}{2b}\right)\right) - \frac{\Delta C}{\varepsilon_o} \tag{3.11}$$

In this form, it is easy to identify the first term in eq. (3.11) as the plate capacitance between the center septum and the horizontal walls, and the second term as the fringing capacitance between the edges of the septum and the side walls. For large gaps, the fringing term approaches $\frac{8}{\pi} \ln 2$, as expected [8].

It is interesting to note that the term in the square brackets in eq. (3.11) is the identical formula given by T.-S. Chen [8] and originally derived by S.B. Cohn [9]. Cohn's formula was derived assuming that the width of the center septum, 2w, was very large compared to the plate separation, 2b. This is equivalent to assuming that the two edges of the septum do not interact. ΔC, then in eq. (3.11) can be interpreted as a correction term needed to account for the interaction between the two edges. From eq. (3.9) it can be seen that ΔC will be negligibly small if λ is near one (or λ' is near zero) since k is near one. From eq. (2.13) λ'^2 is given approximately by:

$$\lambda'^2 \simeq k'^2 \sinh^4\left(\frac{\pi g}{2b}\right) \tag{3.12}$$

It can be seen from eq. (3.12) that for small gaps, λ' is always much less than one. By using the approximate expression for the modulus, k given by G.M. Anderson [10], it can be shown that for large gaps eq. (3.12) further reduces to:

$$\lambda'^2 \simeq e^{-2\pi \frac{w}{b}} \tag{3.13}$$

From eq. (3.13) it can easily be verified that λ' will be negligibly small, and hence ΔC may be neglected if:

$$\frac{w}{b} \geq \frac{1}{2} \tag{3.14}$$

From eq. (3.3) we have the restriction that $\lambda^2 > \frac{1}{2}$ or equivalently $\lambda'^2 < \frac{1}{2}$. From eq. (3.13) it can be seen that $\lambda'^2 < \frac{1}{2}$ if:

$$\frac{w}{b} \geq \frac{1}{2\pi} \ln 2 \simeq 0.1 \tag{3.15}$$

So for the range: $\frac{1}{10} < \frac{w}{b} < \frac{1}{2}$, ΔC is not negligible and must be calculated using eqs. (3.9), (3.13), and $k \cong 1$.

Using eq. (2.10), the characteristic impedance is found to be:

$$Z_o \cong \frac{\eta_o}{4\left[\frac{a}{b} - \frac{2}{\pi} \ln\left(\sinh \frac{\pi g}{2b}\right)\right] - \frac{\Delta C}{\varepsilon_o}} \tag{3.16}$$

Thus we have obtained approximate expressions for the capacitance and characteristic impedance of the TEM cell. These are given in eqs. (3.8), (3.9), and (3.16). Due to the limitations of the approximations, these formulas are valid for $a/b \geq 1$ and $\frac{w}{b} \geq \frac{1}{2\pi} \ln 2$. The approximate formula for the capacitance given in eq. (3.8) is plotted in figure 3 with a dashed line for $\Delta C = 0$. The exact formula using eqs. (2.11), (2.13), and (2.15) is plotted using a solid line. The two curves agree almost identically except where $w/b < \frac{1}{2}$. This discrepancy can be attributed, however, to the ΔC term which was neglected.

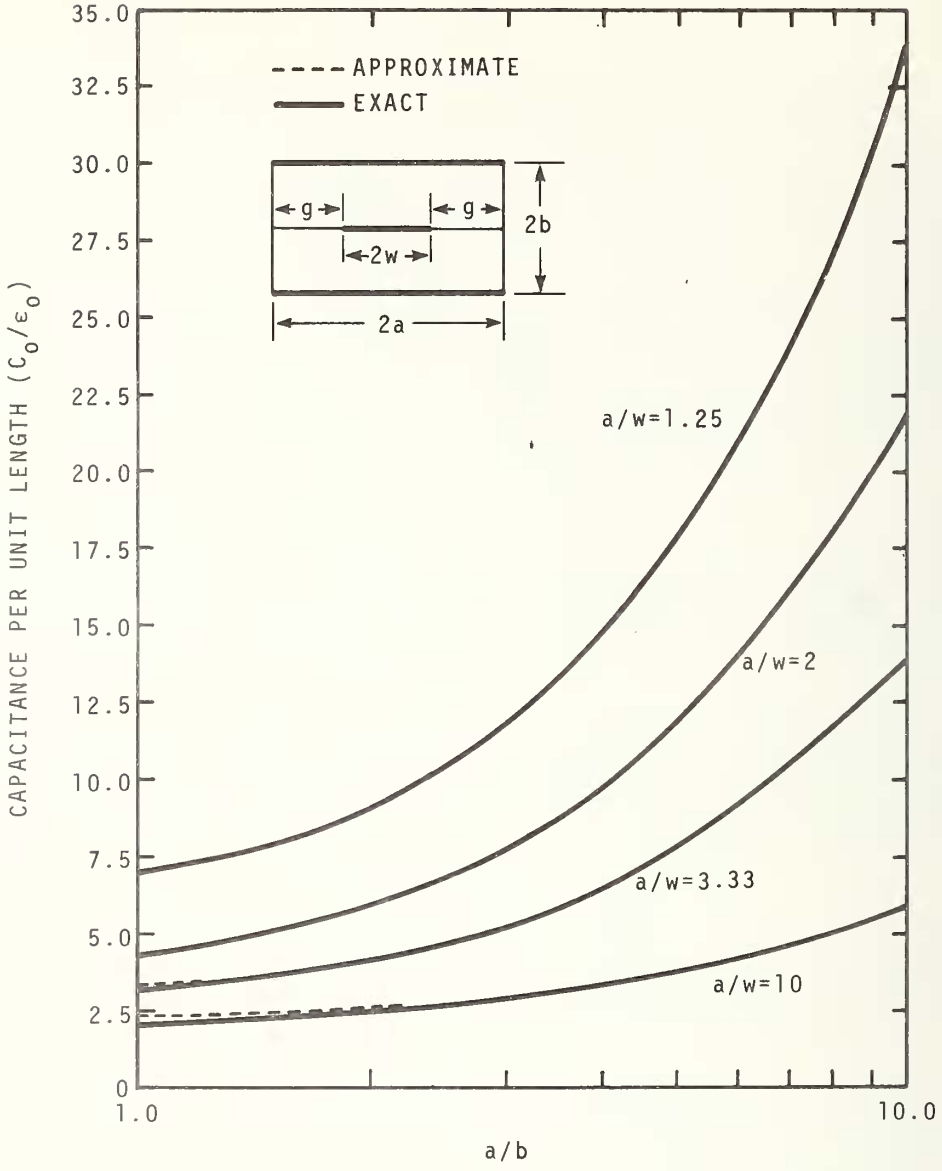

Figure 3. Capacitance per unit length of a TEM cell.

4. RADIATION RESISTANCE OF ELECTRIC AND MAGNETIC DIPOLES IN A TEM CELL

The power carried by the TEM mode of a transmission line that is excited by an elementary electric dipole is given by [11]:

$$P_e = \frac{|A^+|^2 V^2}{Z_o} \tag{4.1}$$

where A^+ is the excitation factor;
V is a unit voltage;
and Z_o is the characteristic impedance.
From Green's theorem, A^+ is given by:

$$A^+ = -\frac{Z_o}{2V^2} \int_\tau \bar{J} \cdot \bar{E}^{(-)} \, dv' \tag{4.2}$$

where $\bar{J}$ is the source current density;
$\bar{E}^{(-)}$ is the electric field of the negative (-z) propagating wave;
and τ is the volume enclosing all sources.

Since our source is an electric dipole, the volume integral in eq. (4.2) reduces to:

$$\int_\tau \bar{J} \cdot \bar{E}^{(-)} \, dv' = E_o(x_o,y_o,z_o) \; I \; \ell_{eff} \cos\theta \tag{4.3}$$

where (x_o,y_o,z_o) is the source point;
θ is the angle between the dipole and the electric field at the source point;
ℓ_{eff} is the effective dipole length;
I is the magnitude of the dipole current;
and E_o is the magnitude of the electric field at the source point.

Using eqs. (4.2) and (4.3), eq. (4.1) can be written as:

$$P_e = Z_o \left(\ell_{eff} \frac{E_o I \cos\theta}{2V} \right)^2 \tag{4.4}$$

If, instead of an electric dipole, our source were a magnetic dipole, then following a similar analysis, the radiated power is given by

$$P_m = Z_o \left(\frac{2\pi A}{\lambda_o} \cdot \frac{E_o I_m \cos\phi}{2V} \right)^2 \tag{4.5}$$

where λ_o is the wavelength;
$A=\pi r^2$ is the area of the loop representing the magnetic dipole;
I_m is the equivalent magnetic current;
and ϕ is the angle between the loop normal and the magnetic field at the source point.

In order to determine the change in the radiation characteristics of the source, we will calculate the ratio of the radiation resistance inside the cell to that in free space. The free space radiation resistances of electric and magnetic dipoles are given in reference [12] as:

$$R_e = \frac{2\pi}{3}\,\eta_o\left(\frac{\ell_{eff}}{\lambda_o}\right)^2 \tag{4.6}$$

$$R_m = \frac{\pi}{6}\,\eta_o\left(\frac{2\pi r}{\lambda_o}\right)^4 \tag{4.7}$$

From eqs. (4.4) and (4.5), the radiation resistances inside the guide are given by:

$$R'_e = \frac{P_e}{I^2} = Z_o\left(\ell_{eff}\,\frac{E_o\cos\theta}{2V}\right)^2 \tag{4.8}$$

$$R'_m = \frac{P_m}{I_m^2} = Z_o\left(\frac{2\pi A}{\lambda_o}\,\frac{E_o\cos\phi}{2V}\right)^2 \tag{4.9}$$

If we define the following, normalized parameters:

$$Z'_o = \frac{Z_o}{\eta_o} \tag{4.10}$$

$$\tilde{E} = \frac{E_o}{V/b} \tag{4.11}$$

then the ratios, Q_e and Q_m, of the radiation resistances are respectively:

$$Q_e = \frac{R'_e}{R_e} = \frac{3\pi}{2}\,Z'_o\left(\frac{\tilde{E}\cos\theta}{k_o b}\right)^2 \tag{4.12}$$

$$Q_m = \frac{R'_m}{R_m} = \frac{3\pi}{2}\,Z'_o\left(\frac{\tilde{E}\cos\phi}{k_o b}\right)^2 \tag{4.13}$$

where $k_o = 2\pi/\lambda_o$. Thus, in order to determine the "correction factors," Q_e and Q_m, which determine the change in the radiation characteristics of dipole sources inside a TEM cell as compared to free space, we need to know the squared magnitude of the electric field E_o, at the dipole location. An analytical expression for the electric field squared is shown in Appendix B as:

$$E_o^2 = \left(\frac{Vm'}{K(\alpha')}\right)^2\left|\frac{dn^2(m'z)}{sn^2(m'w) - sn^2(m'z)}\right| \tag{4.14}$$

where

$$\alpha' = [1 - \alpha^2]^{\frac{1}{2}}; \tag{4.15}$$

$$\alpha = sn(m'w,k); \tag{4.16}$$

$$\frac{a}{b} = \frac{K(k)}{K(k')}; \tag{4.17}$$

$$m' = \frac{K(k)}{a}; \tag{4.18}$$

and

$$z = x + iy;$$

where x and y indicate the location of the dipole as measured from the center of the TEM cell in the transverse plane. Thus, $\tilde{E}$ in eqs. (4.12) and (4.13) is given by:

$$\tilde{E} = \left(\frac{bm'}{K(\alpha')}\right)\left|\frac{dn^2(m'z)}{sn^2(m'w) - sn^2(m'z)}\right|^{1/2} \tag{4.19}$$

We further note that eqs. (4.12) and (4.13) are very similar. In fact, if we were to average cos θ and cos φ they would be identical. That is,

$$\langle Q_e \rangle = \langle Q_m \rangle \equiv Q_o/(k_o b)^2 \tag{4.20}$$

where

$$Q_o = \frac{3\pi}{4} Z_o' \tilde{E}^2 \tag{4.21}$$

So that the same correction factor can be applied whether the dipole is electric or magnetic. It is interesting to note that this is the same result obtained by D.M. Kerns in his analysis of dipoles located in an ordinary coaxial line [13]. His result for the correction factor also contains the same (1/frequency)^2 dependence, but the constant Q_o which contains the geometrical constants characteristic of the particular transmission line (through Z_o), is different. Equation (4.20) is plotted in figure 4 and shows how the radiation resistance is

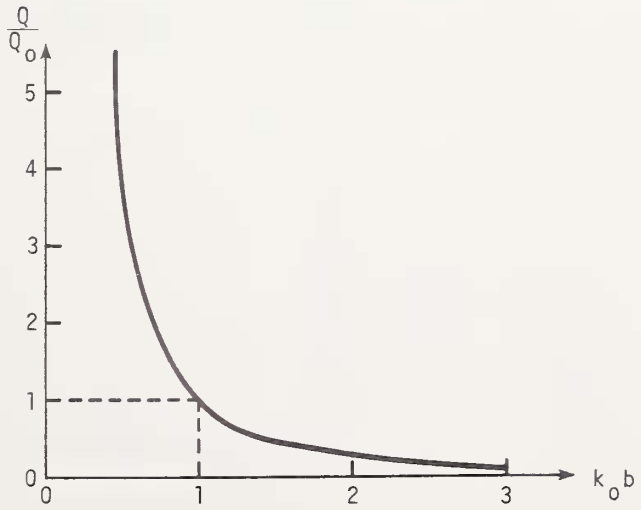

Figure 4. Correction factor as a function of frequency.

reduced as the frequency is increased. Values of Q_o are included in tables 1-2 for dipoles located at various places inside a TEM cell. Each table corresponds to a different TEM cell geometry.

Table 1

Q_o, the ratio of the radiation resistance inside the TEM cell to that in free space for $k_o b = 1$. Dimensions of the TEM cell: a = 25 cm, b = 25 cm, w = 20.64 cm.

y(cm)	0	5	10	15	20	25
y=b→25	0.220	0.205	0.158	0.091	0.027	0.000
20	0.236	0.222	0.181	0.119	0.057	0.031
15	0.248	0.277	0.255	0.217	0.172	0.150
10	0.357	0.365	0.390	0.435	0.482	0.497
5	0.432	0.460	0.567	0.866	1.507	1.696
0	0.465	0.503	0.665	1.281	14.322	4.216

x(cm)

Center of TEM cell

x=w

x=a

Table 2

Q_o, the ratio of the radiation resistance inside the TEM cell to that in free space for $k_o b = 1$. Dimensions of the TEM cell: a = 25 cm, b = 15 cm, w = 18.025 cm.

y(cm)	0	5	10	15	20	25
y=b→15	0.303	0.291	0.247	0.159	0.051	0.000
12	0.307	0.297	0.259	0.177	0.071	0.020
9	0.318	0.314	0.294	0.238	0.140	0.087
6	0.332	0.336	0.350	0.367	0.291	0.217
3	0.344	0.356	0.412	0.622	0.642	0.403
0	0.349	0.364	0.441	0.901	1.262	0.512

x(cm)

Center of TEM cell

x=w

x=a

5. SUMMARY AND CONCLUDING REMARKS

We have calculated in this report the exact capacitance and characteristic impedance of a TEM cell, as given by eqs. (2.11) and (2.16). In addition, approximate formulas given by eqs. (3.8), (3.9), and (3.16) were obtained which agree very closely with the exact results. Finally, the electric field distribution of the TEM mode, given by eq. (4.14), was obtained analytically and was used to derive expressions for the radiation resistance of simple dipoles located inside a TEM cell as given in eqs. (4.8) and (4.9). These expressions, when compared to their free-space counterparts, allows one to evaluate the change in the radiation characteristics of those sources which can be modeled by dipoles when located inside the TEM cell as compared to free-space.

How can these results be used to interpret measurements made on a practical source radiating inside a TEM cell, such as a piece of electronic equipment? When can a practical source be modeled by a collection of elementary dipoles? If the source can be modeled by a collection of dipoles, how can we determine the magnitudes and directions as well as the type (electric or magnetic) of the dipoles which represent the source? These are all questions which should be asked, and which, as yet, have not been completely answered. We will, however, indicate some of the problems and some ideas that might be used to solve them.

When we model the source by a dipole, we are assuming that the source is "electrically small"; that is, its dimensions are small compared to the operating wavelength. The useful upper frequency limit of the TEM cells used at NBS is typically 100 MHz. At this frequency the wavelength is 3 meters, so that the dimensions of most electronic equipment will be only a fraction of a wavelength and can therefore be modeled by dipoles of both electric and magnetic type. This means, of course, that we are not interested in determining where leaks occur from a piece of equipment since we have assumed a "point" source.

Assume, now, that we have a collection of electric and magnetic dipoles all operating in phase at the same frequency, which is under our control. By superposition, all of the electric dipoles can be combined into one equivalent electric dipole. Similarly, all of the magnetic dipoles can be combined into an equivalent magnetic dipole. We would like to be able to determine the magnitudes and directions of these equivalent dipoles. From eqs. (4.4) and (4.5) the total power radiated is given by:

$$P = P_e + P_m = Z_o \left(\frac{E_o}{2V}\right)^2 \left[(\ell_{eff} \, I \cos\theta)^2 + \left(\frac{2\pi A I_m \cos\phi}{\lambda_o} \right)^2 \right] \qquad (5.1)$$

At low frequencies, eq. (5.1) is dominated by the first term, so that $P \simeq P_e$. At high frequencies, the second term dominates, and $P \simeq P_m$. Therefore, by judiciously choosing the frequency, we can make the source appear as if it were either an electric or magnetic dipole. Whether or not we have chosen a frequency such that the source appears as a single type of dipole and not a "hybrid" dipole should be verified by measuring the power as a function of frequency over a narrow frequency band. The electric dipole will exhibit a characteristic that is independent of frequency, whereas the characteristic of the magnetic dipole will increase as the square of the frequency. If we are not able to adjust the frequency so that the source appears as only one type of dipole, then we will have to take measurements at two selected frequencies and fit the data to eq. (5.1); so that even in this case, the separation of the contributions from the electric and magnetic dipoles is not a problem.

Now assume that we are able to obtain a single dipole source by adjusting the frequency. By measuring the power, we can determine the magnitude of the dipole moment times the cosine of some angle; $(\ell_{eff} I) \cos \theta$ for the electric dipole, and $(AI_m) \cos \phi$ for the magnetic dipole. In order to separate the angular dependence from the dipole magnitude we can perform the following experiment.

(1) Rotate the source until the radiated power is zero, thus aligning the electric or magnetic dipole perpendicularly to the respective field.
(2) Rotate the source about the longitudinal axis of the TEM cell (z-axis). If the power radiated does not remain zero, return the source to its original position.
(3) Rotate the source slightly about the x axis for magnetic dipoles or the y axis for electric dipoles.
(4) Repeat steps (2) and (3) until the radiated power remains zero upon rotation about the z-axis.
(5) The dipole is then aligned along the z-axis.

Thus, we can rotate the electric or magnetic dipole 90° around the x or y axis respectively, and obtain $\cos \theta = 1$ or $\cos \phi = 1$. With the dipole so oriented, we can measure the magnitude of the dipole moment by measuring the power radiated.

The procedure just described is more complicated if we have both an electric and a magnetic dipole. In this case, we may not be able to obtain a null in the power by rotating the source. By taking measurements as a function of frequency and rotation angle of the source, however, we can separate the contributions from both the electric and magnetic dipoles, as well as their respective orientations. Thus, having found the equivalent dipoles that represent the source, we are able to predict the radiation characteristics of the source in free space. It should also be noted that in this report we have addressed ourselves to the problem of radiated emissions testing of electrically small devices; by reciprocity, however, the results are applicable also to the problem of susceptibility testing.

The usefulness of the technique just described hinges on the validity of the following assumptions that were made initially. (1) The equivalent dipoles that represent the source have dipole moments that are constants, independent of frequency. (2) The directions of the dipoles are not a function of frequency. (3) The electric and magnetic dipoles operate in phase at the same frequency, and (4) the operating frequency is under our control. These assumptions will now be examined.

In order to understand why it seems reasonable to model a practical source by an equivalent electric and magnetic dipole operating in phase at the same frequency, we will borrow some of the results from the theory of excitation of waveguides by small apertures [14]. We will consider a practical source to consist of an electrically small conducting box housing low-frequency AC circuits. The box can have numerous apertures through which electromagnetic energy may radiate; however, we restrict these apertures to be small compared to the size of the conducting box. The coupling through a small aperture can be modeled by replacing the aperture by an equivalent electric and magnetic dipole. The magnitude of the electric dipole is proportional to the normal electric field that would be present at the aperture assuming the aperture is replaced by a perfect conductor. Similarly, the magnitude of the magnetic dipole is proportional to the tangential magnetic field that would exist at the aperture. It seems reasonable to assume that at the apertures no normal electric fields would exist, since this would imply that a net accumulation of charge would exist inside the box. However, there could exist tangential magnetic fields as a result of any current loops in the circuitry. Thus, we will model the apertures by magnetic dipoles only. These dipoles will induce currents and charges on the outside surface of the conducting box, which can, in turn, be modeled by an equivalent electric dipole and a magnetic dipole. These dipoles will obviously not have magnitudes that are independent of frequency; however, at each frequency, the relationship between the magnitude of the electric and magnetic dipole will remain fixed, if we assume that the box contains only one source which induces both dipoles. Since the box is electrically small and contains only one source, the equivalent dipoles will also operate in phase. By the same argument, their directions will not be a function of frequency. Therefore, we can separate the contribution to the total power radiated from each dipole as described previously by measuring the power radiated at two selected frequencies. Since in some cases we do not have the operating frequency under our control, this will not always be possible unless our source radiates at more than one frequency, or we know a priori from physical grounds that the source can be modeled by only one type of dipole.

6. REFERENCES

[1] Adams, J.W., Electromagnetic Interference Measurement Program at the National Bureau of Standards, USNC/URSI, Commissions I-VIII, Annual Meeting, p. 33 (Oct. 20-23, 1975).

[2] Crawford, M. L., Generation of standard EM field using TEM transmission cells, IEEE Trans. on Electromagnetic Compatibility, EMC-16, No. 4 (Nov. 1974).

[3] Bowman, F., Introduction to Elliptic Functions with Applications, Chapter II (Dover Publ. Inc., New York, 1961).

[4] Ibid., Chapter I.

[5] Abramowitz and Stegun, Eds., Handbook of Mathematical Functions, 5th Ed., p. 612 (Dover Publ. Inc., New York, 1968).

[6] Ibid., Sec. 17.6, p. 598.

[7] Whittaker, E.T. and Watson, G.N., A Course of Modern Analysis, 4th Ed., p. 486 (Cambridge Univ. Press, 1969).

[8] Chen, T.-S., Determination of the capacitance, inductance, and characteristic impedance of rectangular lines, IRE Trans. on MTT, MTT-8, No. 5, 510-519 (Sept. 1960).

[9] Cohn, S.B., Shielded coupled-transmission line, IRE Trans. on MTT, MTT-3, No. 5, 29-38 (Oct. 1955).

[10] Anderson, G. M., The calculation of the capacitance of coaxial cylinders of rectangular cross-section, AIEE Trans., 69, pt. II, 728-731 (1950).

[11] Collin, R.E., Field Theory of Guided Waves, pp. 200-204 (McGraw-Hill, New York, 1960).

[12] Ramo, Whinnery and Van Duzer, Fields and Waves in Communication Electronics, pp. 645, 657 (Wiley, New York, 1967).

[13] Kerns, D.M., unpublished work (Aug. 1965).

[14] Collin, R.E., op cit., pp. 285-302.

[15] Walker, M., The Schwarz-Christoffel Transformation and Its Applications -- A Simple Exposition (Dover Publ. Inc., New York, 1964).

[16] Bowman, F., op cit., p. 58.

[17] Bowman, F., op cit., p. 57.

[18] Churchill, R.V., Complex Variables and Applications, 2nd Ed., p. 209 (McGraw-hill, New York, 1960).

[19] Abramowitz and Stegun, op cit., Sec. 17.6, p. 598, Sec. 16.4, p. 571.

[20] Abramowitz and Stegun, op cit., Sec. 16.21, p. 575.

APPENDIX A
Calculation of the Capacitance of a TEM Cell

A cross-section view of the TEM cell is shown in figure 5 with an x-y coordinate system superimposed.

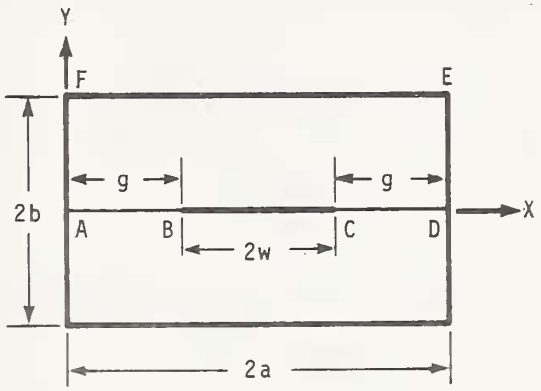

Figure 5. Cross-section of a TEM cell.

The center septum of width 2w is located symmetrically inside the cell of height 2b and width 2a and is assumed to have negligible thickness. In addition, the septum is located a distance g from each vertical side wall and is embedded in a homogeneous dielectric of permittivity, ε_o. For convenience, some key points in the cell have been labeled A through F. The reason for choosing an unsymmetrically located coordinate system is to facilitate obtaining the approximate formula for the capacitance given in section 3.

To determine the capacitance, the method of conformal transformation will be used, whereby the structure in figure 5 is transformed into a simpler configuration whose capacitance is already known. Since it is well known that capacitance is invariant under a conformal transformation, the formula obtained will also be applicable to the TEM cell.

Since we have symmetry with respect to the septum, we will calculate the capacitance between the upper plate, A-F-E-D and the center septum B-C. The total capacitance is then twice this figure, since we have effectively two capacitors in parallel. The region A-D-E-F may be mapped into the upper-half of a complex t-plane via the Schwarz-Christoffel transformation [15] which, due to symmetry, can be expressed in terms of Jacobian elliptic functions. The transformation is given by [16]:

$$mz = \int_o^t \frac{dt}{[4t(1-t)(1-k^2t)]^{\frac{1}{2}}} \qquad (A.1)$$

or alternatively by:

$$t = sn^2(mz,k) \qquad (A.2)$$

where sn is a Jacobian elliptic function of modulus, k;

$$m = \frac{K(k')}{b}; \tag{A.3}$$

and

$$z = x + iy. \tag{A.4}$$

Here K(k) and K(k') are complete elliptic integrals of the first kind of moduli k and k' respectively and:

$$k' = [1 - k^2]^{\frac{1}{2}} \tag{A.5}$$

The modulus k can be determined from the requirement that:

$$\frac{K(k)}{K(k')} = \frac{2a}{b} \tag{A.6}$$

Under the transformation given by eq. (A.2), the region, A-D-E-F, in the z-plane is mapped into the upper half of the t-plane as shown in figure 6.

Figure 6. Complex t-plane.

Using eq. (A.2) and elliptic function identities, α_o and β_o can be calculated as:

$$\alpha_o = sn^2 mg = sn^2 \xi \tag{A.7}$$

$$\beta_o = sn^2 m(2a-g) = cn^2 \xi / dn^2 \xi \tag{A.8}$$

where

$$\xi \equiv mg \tag{A.9}$$

and cn and dn are also Jacobian elliptic functions all of which have modulus, k. For convenience, we now make an intermediate transformation from the t-plane to a complex u-plane defined by:

$$u = \frac{\beta_o}{t}\left(\frac{t - \alpha_o}{\beta_o - \alpha_o}\right) \tag{A.10}$$

The u-plane is shown in figure 7.

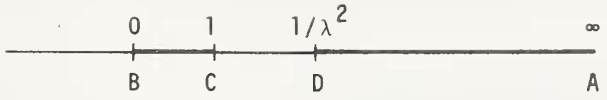

Figure 7. Complex u-plane.

λ in figure 7 can be found using eq. (A.10) and substituting t = 1. Thus:

$$\frac{1}{\lambda^2} = \beta_o \left[\frac{1 - \alpha_o}{\beta_o - \alpha_o} \right] \tag{A.11}$$

Substituting for α_o and β_o from eq. (A.7) and eq. (A.8), we obtain:

$$\lambda^2 = \frac{cn^2\xi - sn^2\xi\, dn^2\xi}{cn^2\xi[1-sn^2\xi]} \tag{A.12}$$

Using elliptic function identities, eq. (A.12) reduces to:

$$\lambda^2 = 1 - k'^2 \left[\frac{sn\ \xi}{cn\ \xi} \right]^4 \tag{A.13}$$

and defining a complementary modulus, λ' as:

$$\lambda' = [1 - \lambda^2]^{\frac{1}{2}} \tag{A.14}$$

We have from eqs. (A.13) and (A.14):

$$\lambda' = k' \left[\frac{sn\ \xi}{cn\ \xi} \right]^2 \tag{A.15}$$

In the final transformation, we map the upper half of the u-plane into a rectangular region in a complex χ-plane. The transformation is given by:

$$u = sn^2(\chi, \lambda) \tag{A.16}$$

and the χ-plane is shown in figure 8.

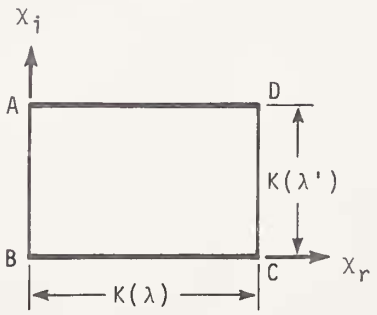

Figure 8. Complex χ-plane.

From figure 8, it is evident that the capacitance is just given by the ordinary parallel plate capacitor formula, that is:

$$C = \frac{\varepsilon_o A_o}{d} \tag{A.17}$$

where A_o is the cross-sectional area;
d is the plate spacing;
and ε_o is the permittivity of free space.

Substituting for A_o and d in terms of $K(\lambda)$ and $K(\lambda')$ we obtain:

$$\frac{C}{\varepsilon_o} = \frac{K(\lambda)}{K(\lambda')} \tag{A.18}$$

where C is now interpreted as the capacitance per unit length. Therefore, the total capacitance of the TEM cell per unit length is just twice that given by eq. (A.18).

$$\frac{C_o}{\varepsilon_o} = 2\,\frac{K(\lambda)}{K(\lambda')} \tag{A.19}$$

APPENDIX B

Calculation of the Electric Field Distribution Inside a TEM Cell

In order to evaluate eqs. (4.12) and (4.13), we need to calculate the magnitude of the electric field, E_o, inside the guide. This is most easily done using a different coordinate system as well as a Schwarz-Christoffel transformation similar to that used in Appendix A. A cross-section view of the TEM cell is shown in figure 9 with a symmetrical x-y coordinate system superimposed.

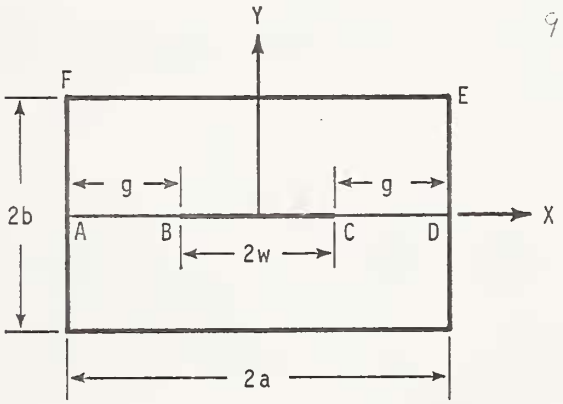

Figure 9. Cross-section of a TEM cell.

The region A-D-E-F can be mapped into the upper-half of a complex t_o-plane via the following transformation [17]:

$$t_o = sn(m'z,k) \tag{B.1}$$

where

$$m' = \frac{K(k)}{a} = \frac{K(k')}{b} \tag{B.2}$$

Note that this transformation is not the same as the one used in Appendix A to solve for the capacitance, since a different coordinate system was used. The symbols used in this appendix should not be confused with those in Appendix A.

The complex t_o-plane is shown in figure 10.

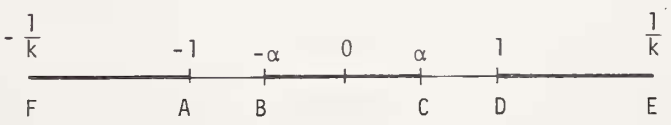

Figure 10. Complex t_o-plane.

From eq. (B.1), α is given by:

$$\alpha = sn(m'w,k) \tag{B.3}$$

For convenience, we now make an intermediate transformation from the t_o-plane to a complex u_o-plane defined by:

$$u_o = t_o/\alpha \tag{B.4}$$

The u_o-plane is shown in figure 11.

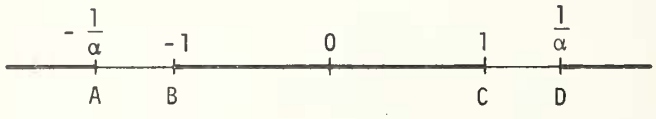

Figure 11. Complex u_o plane.

Finally, we map the upper-half of the u_o-plane into a complex χ_o-plane defined by:

$$u_o = sn(\chi_o,\alpha) \tag{B.5}$$

The χ_o-plane is shown in figure 12.

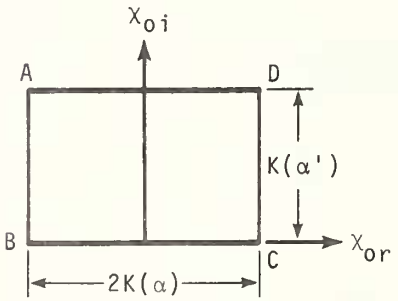

Figure 12. Complex χ_o-plane.

In order to calculate the electric field, we must find the complex potential, F, which is given by [18]:

$$F = \phi(\chi_o) + i\psi(\chi_o) \tag{B.6}$$

where $\phi(\chi_o)$ is the potential function;
$\psi(\chi_o)$ is the stream function;
and F satisfies the Cauchy-Riemann equations.
In addition the potential $\phi(\chi_o)$ must satisfy the following boundary conditions:

$\phi(\chi_o) = 0$ on BC

and $\phi(\chi_o) = V$ on AD.

It is easily verified that the following solution satisfies all of the above requirements:

$$\phi(\chi_o) = \frac{V\chi_{oi}}{K(\alpha')} \tag{B.7}$$

and

$$\psi(\chi_o) = -\frac{V\chi_{or}}{K(\alpha')} \tag{B.8}$$

where

$$\chi_o = \chi_{or} + i\chi_{oi}$$

The electric field, E, is defined by:

$$E = -\nabla\phi = -\left(\frac{\partial}{\partial x}\phi + i\frac{\partial}{\partial y}\phi\right)$$

$$= -\left(\frac{\partial}{\partial x}\phi - i\frac{\partial}{\partial x}\psi\right) = \frac{d}{dz}F^* \tag{B.9}$$

The real part of E gives the x-component of the electric field, and the imaginary part of E gives the y-component of the electric field. $\frac{dF}{dz}$ may be calculated as follows:

$$\frac{dF}{dz} = \frac{dF}{d\chi_o}\frac{d\chi_o}{du_o}\frac{du_o}{dt_o}\frac{dt_o}{dz} \tag{B.10}$$

Using eq. (B.1) and eq. (B.4) through eq. (B.8), $\frac{dF}{dz}$ may be evaluated as:

$$\frac{dF}{dz} = \frac{-iVm'\,dn(m'z)}{K(\alpha')[P_o(z)]^{\frac{1}{2}}} \tag{B.11}$$

where

$$P_o(z) = [sn^2(m'w) - sn^2(m'z)] \tag{B.12}$$

Thus, the magnitude-squared of the electric field, E_o^2 is given by:

$$E_o^2 = \left(\frac{Vm'}{K(\alpha')}\right)^2 \left|\frac{dn^2(m'z)}{sn^2(m'w) - sn^2(m'z)}\right| \tag{B.13}$$

It is easy to see from eq. (B.13) that for $z = \pm w$, E_o^2 goes to infinity as expected from the edge condition.

Equation (B.11) was evaluated numerically for some typical TEM cell geometries and used to calculate the x and y components of the electric field, as well as the magnitude and polarization angle of the electric field defined by:

$$\theta = \arctan\left(\frac{E_y}{E_x}\right) \tag{B.14}$$

These results are included in tables 3 through 10 where all field quantities have been normalized to V/b. In addition, the relative electric field distribution is plotted in figure 13. The top graph in that figure contains experimental data measured by M.L. Crawford [2] for comparison.

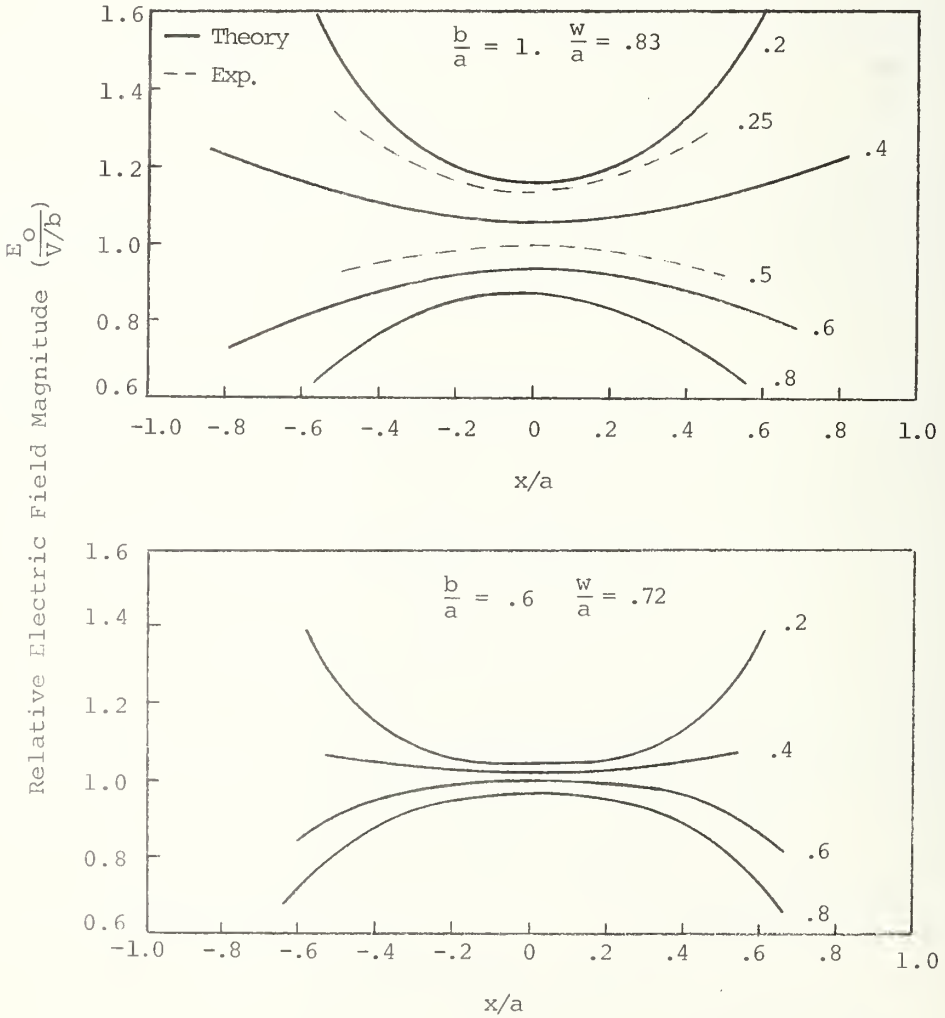

Figure 13. Relative electric field distribution inside a TEM cell. Parameter indicates distance from the center septum (y/b).

Table 3

x-component of the electric field in a TEM cell of dimensions: a = 25 cm, b = 25 cm, w = 20.64 cm normalized to V/b.

y(cm)	0	5	10	15	20 (x=w)	25 (x=a)
y=b→25	0.000	0.000	0.000	0.000	0.000	0.000
20	0.000	0.060	0.129	0.208	0.278	0.307
15	0.000	0.108	0.245	0.422	0.600	0.680
10	0.000	0.127	0.311	0.620	1.029	1.237
5	0.000	0.090	0.248	0.647	1.684	2.285
0	0.000	0.000	0.000	0.000	0.000	3.603

x(cm)

Center of TEM cell

Table 4

y-component of the electric field in a TEM cell of dimensions: a = 25 cm, b = 25 cm, w = 20.64 cm normalized to V/b.

y(cm)	0	5	10	15	20 (x=w)	25 (x=a)
y=b→25	0.824	0.793	0.698	0.530	0.289	0.000
20	0.853	0.825	0.736	0.568	0.315	0.000
15	0.935	0.917	0.852	0.699	0.410	0.000
10	1.049	1.052	1.051	0.977	0.652	0.000
5	1.153	1.186	1.298	1.499	1.343	0.000
0	1.196	1.245	1.431	1.986	6.640	0.000

x(cm)

Center of TEM cell

Table 5

Magnitude of the electric field in a TEM cell of dimensions: a = 25 cm, b = 25 cm, w = 20.64 cm normalized to V/b.

y(cm)						
y=b→25	0.824	0.793	0.698	0.530	0.289	0.000
20	0.853	0.827	0.747	0.605	0.420	0.307
15	0.935	0.924	0.886	0.817	0.727	0.680
10	1.049	1.060	1.096	1.157	1.218	1.237
5	1.153	1.189	1.321	1.633	2.154	2.285
0	1.196	1.245	1.431	1.986	6.640	3.603
	0	5	10	15	20 (x=w)	25 (x=a)

x(cm)

Center of TEM cell

Table 6

Polarization angle of the electric field in degrees in a TEM cell of dimensions: a = 25 cm, b = 25 cm, w = 20.64 cm.

y(cm)						
y=b→25	90.00	90.00	90.00	90.00	90.00	--
20	90.00	85.86	80.05	69.89	48.54	00.00
15	90.00	83.27	73.97	58.89	34.35	00.00
10	90.00	83.14	73.50	57.60	32.36	00.00
5	90.00	85.64	79.20	66.67	38.56	00.00
0	90.00	90.00	90.00	90.00	90.00	00.00
	0	5	10	15	20 (x=w)	25 (x=a)

x(cm)

Center of TEM cell

Table 7

x-component of the electric field in a TEM cell of dimensions: a = 25 cm, b = 15 cm, w = 18.025 cm normalized to V/b.

y(cm)						
y=b→15	0.000	0.000	0.000	0.000	0.000	0.000
12	0.000	0.024	0.067	0.143	0.220	0.249
9	0.000	0.040	0.121	0.284	0.462	0.517
6	0.000	0.043	0.141	0.410	0.763	0.817
3	0.000	0.028	0.101	0.440	1.247	1.112
0	0.000	0.000	0.000	0.000	1.969	1.254
	0	5	10	15	20	25 x(cm)

Center of TEM cell

x=w

x=a

Table 8

y-component of the electric field in a TEM cell of dimensions: a = 25 cm, b = 15 cm, w = 18.025 cm normalized to V/b.

y(cm)						
y=b→15	0.966	0.946	0.872	0.698	0.394	0.000
12	0.972	0.956	0.890	0.724	0.411	0.000
9	0.989	0.981	0.944	0.807	0.464	0.000
6	1.010	1.015	1.028	0.979	0.557	0.000
3	1.028	1.046	1.120	1.311	0.645	0.000
0	1.035	1.058	1.164	1.664	0.000	0.000
	0	5	10	15	20	25 x(cm)

Center of TEM cell

x=w

x=w

Table 9

Magnitude of the electric field in a TEM cell of dimensions: a = 25 cm, b = 15 cm, w = 18.025 cm normalized to V/b.

y(cm)						
y=b→15	0.966	0.946	0.872	0.698	0.394	0.000
12	0.972	0.956	0.892	0.738	0.466	0.249
9	0.989	0.982	0.951	0.856	0.655	0.517
6	1.010	1.016	1.038	1.062	0.945	0.817
3	1.028	1.046	1.125	1.383	1.404	1.112
0	1.035	1.058	1.164	1.664	1.969	1.254
	0	5	10	15	20	25 x(cm)

Center of TEM cell

x=w x=a

Table 10

Polarization angle of the electric field in degrees in a TEM cell of dimensions: a = 25 cm, b = 15 cm, w = 18.025 cm.

y(cm)						
y=b→15	90.00	90.00	90.00	90.00	90.00	--
12	90.00	88.58	85.68	78.80	61.76	00.00
9	90.00	87.66	82.70	70.61	45.12	00.00
6	90.00	87.60	82.20	67.26	36.15	00.00
3	90.00	88.48	84.82	71.43	27.36	00.00
0	90.00	90.00	90.00	90.00	90.00	00.00
	0	5	10	15	20	25 x(cm)

Center of TEM cell

x=w x=a

APPENDIX C

Numerical Evaluation of Complete Elliptic Integrals and Jacobian Elliptic Functions

The method used to evaluate elliptic functions and elliptic integrals is given in reference [19], a summary of which follows. Assuming that the modulus of the particular function desired is k, we begin by defining the following:

$$a_o = 1 \qquad b_o = k' \qquad c_o = k \tag{C.1}$$

Then we set up an Arithmetic-Geometric Mean (AGM) table defined recursively as follows:

$$\begin{aligned}
a_1 &= \tfrac{1}{2}(a_o+b_o) & b_1 &= (a_o b_o)^{\frac{1}{2}} & c_1 &= \tfrac{1}{2}(a_o-b_o) \\
a_2 &= \tfrac{1}{2}(a_1+b_1) & b_2 &= (a_1 b_1)^{\frac{1}{2}} & c_2 &= \tfrac{1}{2}(a_1-b_1) \\
&\vdots & &\vdots & &\vdots \\
a_N &= \tfrac{1}{2}(a_{N-1}+b_{N-1}) & b_N &= (a_{N-1} b_{N-1})^{\frac{1}{2}} & c_N &= \tfrac{1}{2}(a_{N-1}-b_{N-1})
\end{aligned}$$

Stopping at n = N when $c_N = 0$ to the degree of accuracy required.

The complete elliptic integral K(k) is then given by:

$$K(k) = \frac{\pi}{2a_N} \tag{C.2}$$

The Jacobian elliptic functions, sn(ξ), cn(ξ), and dn(ξ) can be determined by calculating ϕ_N in degrees where

$$\phi_N = 2^N a_N \xi \frac{180^\circ}{\pi} \tag{C.3}$$

and then computing recursively, ϕ_{N-1}, ϕ_{N-2}, $\cdots$ ϕ_1, ϕ_o by using:

$$\sin(2\phi_{n-1}-\phi_n) = \frac{c_n}{a_n} \sin \phi_n \tag{C.4}$$

The Jacobian elliptic functions are then given by:

$$sn(\xi,k) = \sin \phi_o \tag{C.5}$$

$$cn(\xi,k) = \cos \phi_o \tag{C.6}$$

$$dn(\xi,k) = \frac{\cos \phi_o}{\cos(\phi_1-\phi_o)} \tag{C.7}$$

In eqs. (C.5) through (C.7), the argument, ξ, was assumed to be real. If the argument is complex then the following formulas from reference [20] can be used.

$$sn(\xi,k) = \frac{s \cdot d_1 + ic \cdot d \cdot s_1 \cdot c_1}{c_1^2 + k^2 \cdot s^2 \cdot s_1^2} \tag{C.8}$$

$$cn(\xi,k) = \frac{c \cdot c_1 - is \cdot d \cdot s_1 \cdot d_1}{c_1^2 + k^2 \cdot s^2 \cdot s_1^2} \tag{C.9}$$

$$dn(\xi,k) = \frac{d \cdot c_1 \cdot d_1 - ik^2 \cdot s \cdot c \cdot s_1}{c_1^2 + k^2 \cdot s^2 \cdot s_1^2} \tag{C.10}$$

where $\xi = \xi_r + i\xi_i$

and $s = sn(\xi_r,k)$ $\quad s_1 = sn(\xi_i,k')$

$c = cn(\xi_r,k)$ $\quad c_1 = cn(\xi_i,k')$

$d = dn(\xi_r,k)$ $\quad d_1 = dn(\xi_i,k')$

Two Fortran subroutines, AGM and SNCNDN, were used to perform the calculations described in this appendix. When AGM(K) is called, the AGM table described above is defined. SNCNDN(X,SN,CN,DN) can then be called with real argument X to return the functions desired. A copy of these subroutines follows.

```
      SUBROUTINE AGM(K)
      COMMON A(20),B(20),C(20),L
      REAL K
      A(1)=1.
      B(1)=SQRT(1.-K*K)
      C(1)=K
      DO 10 I=2,20
      A(I)=.5*(A(I-1)+B(I-1))
      B(I)=SQRT(A(I-1)*B(I-1))
      C(I)=.5*(A(I-1)-B(I-1))
      IF(C(I).LT.1.E-6) GOTO 30
   10 CONTINUE
      PRINT 20
   20 FORMAT(1X,*AGM FAILED TO CONVERGE IN 20 ITERATIONS*)
   30 L=I
      RETURN
      END
```

```
      SUBROUTINE SNCNDN(X,SN,CN,DN)
      COMMON A(20),B(20),C(20),L
      DIMENSION P(20)
      P(L)=A(L)*X*2.**(L-1)
      I=L
   10 P(I-1)=.5*(ASIN((C(I)/A(I))*SIN(P(I)))+P(I))
      I=I-1
      IF(I.NE.0) GOTO 10
      SN=SIN(P(1))
      CN=COS(P(1))
      DN=CN/COS(P(2)-P(1))
      RETURN
      END
```

NBS-114A (REV. 7-73)

U.S. DEPT. OF COMM. BIBLIOGRAPHIC DATA SHEET	1. PUBLICATION OR REPORT NO. NBSIR 75-829	2. Gov't Accession No.	3. Recipient's Accession No.

4. TITLE AND SUBTITLE

RADIATION CHARACTERISTICS OF DIPOLE SOURCES LOCATED INSIDE A RECTANGULAR, COAXIAL TRANSMISSION LINE

5. Publication Date: January 1976

6. Performing Organization Code: 276.00

7. AUTHOR(S): John C. Tippet and David C. Chang

8. Performing Organ. Report No.: NBSIR 75-829

9. PERFORMING ORGANIZATION NAME AND ADDRESS

NATIONAL BUREAU OF STANDARDS
DEPARTMENT OF COMMERCE
WASHINGTON, D.C. 20234

10. Project/Task/Work Unit No.: 2768281

11. Contract/Grant No.:

12. Sponsoring Organization Name and Complete Address *(Street, City, State, ZIP)*

Same as Item 9.

13. Type of Report & Period Covered:

14. Sponsoring Agency Code:

15. SUPPLEMENTARY NOTES

16. ABSTRACT *(A 200-word or less factual summary of most significant information. If document includes a significant bibliography or literature survey, mention it here.)*

When making EMC measurements inside a shielded enclosure, the radiation characteristics of the device being tested changes. In this report the change in radiation resistance of dipole sources located inside a National Bureau of Standards TEM transmission cell is determined. In many cases a practical device can be modeled by dipole sources. In these cases, the analysis allows one to predict the device's radiation characteristics in other environments, e.g., free space.

17. KEY WORDS *(six to twelve entries; alphabetical order; capitalize only the first letter of the first key word unless a proper name; separated by semicolons)* EMC measurements; radiation resistance; rectangular coax; shielded strip line; TEM cell.

18. AVAILABILITY

[x] Unlimited

[ ] For Official Distribution. Do Not Release to NTIS

[ ] Order From Sup. of Doc., U.S. Government Printing Office Washington, D.C. 20402, SD Cat. No. C13

[X] Order From National Technical Information Service (NTIS) Springfield, Virginia 22151

19. SECURITY CLASS (THIS REPORT)	21. NO. OF PAGES
UNCLASSIFIED	33
20. SECURITY CLASS (THIS PAGE)	22. Price
UNCLASSIFIED	$3.75

USCOMM-DC 29042-P74

USCOMM - ERL